Ab initio calculation of the lattice distortions induced by substitutional Ag^- and Cu^- impurities in alkali halide crystals.

Andrés Aguado, José M. López, and Julio A. Alonso
Departamento de Física Teórica, Facultad de Ciencias, Universidad de Valladolid, 47011 Valladolid, Spain
()

An *ab initio* study of the doping of alkali halide crystals (AX: A = Li, Na, K, Rb; X = F, Cl, Br, I) by ns^2 anions (Ag^- and Cu^-) is presented. Large active clusters with 179 ions embedded in the surrounding crystalline lattice are considered in order to describe properly the lattice relaxation induced by the introduction of substitutional impurities. In all the cases considered, the lattice distortions imply the concerted movement of several shells of neighbors. The shell displacements are smaller for the smaller anion Cu^-, as expected. The study of the family of rock-salt alkali halides (excepting CsF) allows us to extract trends that might be useful at a predictive level in the study of other impurity systems. Those trends are presented and discussed in terms of simple geometric arguments.

I. INTRODUCTION

Most of the luminescent materials presently used in several technological applications[1] involve the doping of a pure ionic crystal, that is substitution of some of the ions by other ions with specific absorption-emission characteristics. The fine details of the absorption-emission spectra, as well as the efficiency and resolution of the scintillator, are determined by the system-specific embedding potential acting on the impurity, which is in turn sensitive to the distortion induced by the impurity on the crystal lattice. Thus, a theoretical understanding and accurate determination of those distortions is of paramount importance, moreover if we realize that their experimental measurement is a difficult task.[2–4]

Two main methods are applied nowadays to model impurity systems: supercell techniques, that exploit the convenience of the Bloch theorem by periodically duplicating a finite region of the crystal around the impurity[5]; and the cluster approach, in which the doped crystal is modeled by a finite cluster centered on the impurity and embedded in a field representing the rest of the host lattice. This cluster approach is the one chosen in the present study, and has been used in the past to study the geometrical and optical properties of doped crystals.[6–32] The cluster (active space) can be studied by using standard quantum-mechanical methods. The rest of the crystal (environment) can be described in several ways. In the simplest and most frequently used approach, the environment is simulated by placing point charges on the lattice sites, but this procedure has to be improved in order to obtain a realistic description of the lattice distortions around the impurity.[9–12,15,18,21,24,26,27,31] Model potentials have been developed to represent the effects of the environment on the active cluster, that include attractive and repulsive quantum-mechanical terms aside from the classical Madelung term,[33] but a problem still remains: the large computational cost of conventional molecular orbital (MO) calculations prevents from performing an exhaustive geometrical relaxation of the lattice around the impurity. In the most accurate MO calculations,[12,24,26,27,29,32] only the positions of the ions in the first shell around the impurity are allowed to relax. However, geometrical relaxations far beyond the first shell of neighbors can be expected. In fact, recent semiempirical simulations of solids,[34–42] performed employing phenomenological potentials,[43–48] have shown the importance of considering appropriate large-scale lattice relaxations in the study of a variety of intrinsic and extrinsic defects in ionic crystals. As we will show below, the systems under study in this paper can not be properly described by simply considering an expansion of the first shell of neighbors around the impurity.

In this contribution we report theoretical calculations of the lattice distortions induced by Ag^- and Cu^- substitutional impurities in 16 alkali halide crystals with the rock-salt structure, namely all those noncontaining cesium. For this purpose we use the *ab initio* Perturbed Ion (PI) model,[49–53] which circunvents the problems mentioned above: (a) The active cluster is embedded in an environment represented by the *ab initio* model potentials of Huzinaga *et al.*[33]; (b) The computational simplicity of the PI model allows for the geometrical relaxation of several coordination shells around the impurity.[15,18,31] Moreover, it allows us to study a whole family of systems in order to look for systematic trends that might be useful in later theoretical studies of doped crystals similar to those here considered.

The remainder of this paper is organized as follows: In Section II we describe the active cluster which has been used to model the doped systems. In Section III we present and discuss the results of the calculations, and Section IV summarizes the main conclusions.

II. CLUSTER MODEL

The *ab initio* Perturbed Ion model is a particular application of the theory of electronic separability of Huzinaga and coworkers[54,55] to ionic solids, in which the basic building blocks are reduced to single ions. The PI model was first developed for perfect crystals.[49] Its application to the study of impurity centers in ionic crystals has been described in refs. 15,18,31, and we refer to those papers for a full account of the method. In brief, an active cluster containing the impurity is considered, and the Hartree-Fock-Roothaan (HFR) equations[56] for each ion in the active cluster are solved in the field of the other ions. The Fock operator includes, apart from the usual intra-atomic terms, an accurate quantum-mechanical crystal potential and a lattice projection operator which accounts for the energy contribution due to the overlap between the wave functions of the ions.[57] The atomic-like HFR solutions are used to describe the ions in the active cluster in an iterative stepwise procedure. The wave functions of the lattice ions external to the active cluster are taken from a PI calculation for the perfect crystal and are kept frozen during the embedded-cluster calculation. Those wave functions are explicitely considered for ions up to a distance d from the center of the active cluster such that the quantal contribution from the most distant frozen shell to the effective cluster energy is less than 10^{-6} hartree. Ions at distances beyond d contribute to the effective energy of the active cluster just through the long-range Madelung interaction, so they are represented by point charges. At the end of the calculation, the ionic wave functions are selfconsistent within the active cluster and consistent with the frozen description of the rest of the lattice. The intraatomic Coulomb correlation, which is neglected at the Hartree-Fock level, is computed as a correction by using the Coulomb-Hartree-Fock (CHF) model of Clementi.[58,59]

In a previous work[31] we employed several active clusters of increasing size and with different embedding schemes to describe the scintillator system Tl^+:NaI. That study was undertaken in order to find the necessary requirements that a cluster model has to fulfill in order to describe properly a doped crystal. Here we just describe the best cluster model between those studied in ref. 31. This active cluster, shown in Figure 1, has 179 ions which correspond to the central impurity (Ag^- or Cu^-) plus twelve coordination shells. Those ions are further split up into two subsets. One is formed by the central impurity plus the first four coordination shells, having a total of 33 ions, and both the wave functions and positions of the ions in this subset are allowed to relax. The lattice positions of the other 146 ions of the active cluster are held fixed during the calculations but their wave functions have been selfconsistently optimized. This is done so that the connection between the region where distortions are relevant and the rest of the crystal is as smooth as possible. In our previous study[31] we showed how an unphysically abrupt connection between those two regions fails in describing properly the lattice distortions induced by the impurity. The ions in the interface region can respond to those distortions by selfconsistently adapting their wave functions to the new potential, and thus contribute to build a more realistic (selfconsistent) environment. The geometrical relaxation around the impurity has been performed by allowing for the independent breathing displacements of each shell of ions, and minimizing the total energy with respect to those displacements until the effective cluster energies are converged up to 1 meV. A downhill simplex algorithm[60] was used. For the ions we have used large STO basis sets, all taken from Clementi-Roetti tables.[61]

The cluster used in this work has been shown to be self-embedding consistent for NaI in our previous work.[31] By this we mean that if the pure crystal is represented by this cluster model (that is, if the central impurity is replaced by the halogen ion corresponding to the pure crystal), the results of the cluster model calculations closely agree with those from a PI calculation for the pure crystal, where all cations (or anions) are equivalent by translational symmetry. The same is true for all the family of alkali halide crystals considered here. Nevertheless, the self-embedding consistency is never complete. In order to supress systematic errors from the distortions calculated with the cluster method, the radial displacements of each shell have been calculated using the following formula:

$$\Delta R_i = R_i(Imp^- : AX) - R_i(X^- : AX), \qquad (1)$$

where R_i (i=1, 2, 3, 4) refer to the radii of the first, second, third, and fourth shells around the impurity in the AX crystal, A = Li, Na, K, Rb, X = F, Cl, Br, I, and $Imp^- = Ag^-$, Cu^-. Thus both systems (pure and doped crystals) are treated in eq. (1) on equal foot with the cluster model, and not with different methodologies, and the calculated distortions are free from that potential source of error. Also, in order to have the correct Madelung potential at the impurity site, the calculations have been performed by employing the experimental lattice constants[62] to describe the geometrically frozen part of the crystals.

The only terms omitted in our description are the dispersion terms (coming from interatomic correlation) and relativistic effects for the heavy ions. Although the importance of both effects increase with atomic number, they are not crucial for the structural properties of the systems studied here. Specifically, Martín Pendás *et al.*[63] have shown that the PI method gives lattice constants and bulk moduli in close agreement with experimental results for all alkali halides. The properties of these crystals under the influence of an applied external pressure, a situation where the importance of interatomic correlation effects increases, are also properly reproduced.

III. RESULTS AND DISCUSSION

The calculated distortions, collected in Table I, are the main quantitative result from our study. For visualization of the trends, however, it is better to display the results in a figure, and this is done in Fig. 2, where we have plotted the distortion of each of the four shells in terms of the empirical cationic radii extracted from ref. 62. Those points corresponding to the same anion have been joined with a line to guide the eye. The figure contains only the results for Ag^- because the trends are the same in the case of the Cu^- impurity. Next we describe, shell by shell, the general trends in Fig. 2:

First shell. This shell is formed by 6 cations in ($\frac{1}{2}$,0,0) crystallographic sites, and undergoes an expansion, as might be expected from the larger size of Ag^- compared to the halogen anions. The impurity anion pushes the neighbor cations to make room for itself in the lattice. The expansion is substantial, with percentage values between 9 and 15 %. In the F salts that expansion is larger the larger the cation size, but this trend is violated in the Cl, Br, and I crystals. If we fix the cation, for K and Rb salts the expansion is larger the smaller the anion (notice that the anion size increases in the order F^-, Cl^-, Br^-, I^-). This rule is inverted in the case of Li salts, whereas Na salts constitute an intermediate case. It should be recognised, nevertheless, that the expansion is almost independent of the halogen element in the Li and Na salts.

Second shell. The displacement of the second shell, formed by 12 anions at ($\frac{1}{2}$,$\frac{1}{2}$,0) positions, is always a small contraction. If we fix the anion, the contraction is larger (absolute value) the larger is cation size. If the cation is fixed, for Na, K and Rb salts the contraction is larger the smaller the anion size. Again this trend is inverted for Li salts.

Third shell. This shell, formed by 8 cations at ($\frac{1}{2}$,$\frac{1}{2}$,$\frac{1}{2}$) sites, experiences a small expansion. If we fix the anion, the expansion is smaller the larger the cation size. If the cation is fixed, there is not a definite trend. In the case of Li and Na salts the expansion increases with the anion size (LiI is an exception). This trend is partially inverted in the case of Rb salts, and for K salts all the expansions are almost identical.

Fourth sell. This shell, formed by 6 anions at (1,0,0) positions, experiences an expansion. That expansion increases with cation size if we fix the anion. If the cation is fixed, in K and Rb salts the expansion is smaller the larger the anion size. In Na salts, NaI is again an exception to this general rule, whereas in Li salts the expansion is almost constant.

In the following we try to find some rationalization for the calculated trends. The working rule still in use nowadays stating that the expansion of the first coordination shell can be approximated by the difference between the ionic radii of the impurity and the substituted ion is somewhat misleading. First of all, the ions in a crystal are not hard spheres, but weakly overlapping soft spheres, so one cannot use values for the ionic radii of ions in vacuum in order to *predict* lattice distortions accurately. In particular, the size of an anion may vary in a nonnegligible way from crystal to crystal. To investigate this, we show $(< r^2 >)^{1/2}$ for F^- in fluoride crystals in Table II, where the expectation value is taken over the outermost orbital of the anion (2p), and is calculated from the crystal-consistent ionic wave functions obtained through a PI calculation on the pure crystals. $r_X = (< r^2 >)^{1/2}$ can be taken as a rough measure of the anion size. We also show the analogous quantity for the 5s orbital of the Ag^- impurity in fluorides. The size of the F^- anion varies by a maximum of 2 %, small compared with the size variation of the Ag^- anion (7 %). Ag^- is more compressible than the halogen anions because its outer electronic shell is an s-shell, while it is a p-shell for the halogens. The same can be said of all the halogens. As the size of the cation decreases, Ag^- is more compressed by the crystal environment. This shows that the standard ionic radii cannot be used for predicting distortions, because their values are a genuine *output* of the selfconsistent process. Nevertheless, though they are not useful for accurate predictions, physical insight tells us that the distortions should be correlated with the size of the ions, in the sense that one always expect that larger impurities induce larger distortions. These should be useful at least at a qualitative level.

In Table III we show the differences

$$\delta = r(Ag^- : AX) - r_X(X^- : AX), \qquad (2)$$

where $r(Ag^-:AX)$ is the radius of the Ag^- impurity in the AX crystal, and $r_X(X^-:AX)$ is the radius of the halogen anion. The differences are expected to be related with the first-shell expansions ΔR_1. The values of δ do not show quantitative agreement with those of ΔR_1. If the anion is fixed, δ increases with the cation size, which is consistent with the main trend in ΔR_1 of fluorides, but does not explain the behavior of other halides. The main trends discussed when the cation is fixed are reproduced for the K and Rb crystals but not for the others. From Figure 1 we can see that the exceptional crystals, concerning the trends in ΔR_1, are LiCl, LiBr, LiI, and NaI. The peculiar feature of those four cases is that anions are much larger than cations: the ratios r_A/r_X are the smallest in the family of alkali halides. In a study of the structures of small alkali halide clusters,[64] it was found that materials with small r_A/r_X have a cluster growing pattern different from the rest. Specifically, those systems showed a marked tendency towards ring-like structures, whereas the others adopt fragments of the rocksalt lattice as their minimum energy structures. The main reason is that anion-anion repulsions are much more important when the ratio r_A/r_X is small. In a recent study, A. Martín Pendás *et al.*[65] have applied the atoms–in–molecules (AIM) theory of Bader[66] to study the topology of the electron density in crystals. They found that the

whole group of alkali halides with rocksalt structure can be divided up into three topological families, called R_1, B_1, and B_2 in that paper, and that the ionic radii are the topological organizers. The R_1 family contains KCl, NaF, KF, RbF, RbBr, RbCl and all the cesium halides. The B_1 family contains KI, KBr, LiF, RbI, NaBr, NaCl and NaI, and the B_2 family contains LiCl, LiBr and LiI. There are constant r_A/r_X lines that isolate each family. The largest values of r_A/r_X are found for family R_1 and the smallest for family B_2, with intermediate values for B_1. NaI is so near the B_2 region that it is not surprising that it behaves in Fig. 2 like the elements of the B_2 family. In the AIM theory the critical points of the electron density scalar field are classified as nuclei, bond points, ring points and cage points.[66] When a bond point is found between two nuclei, a bond is established between the corresponding atoms. In the R_1 family there are just anion-cation bonds.[65] We have found that for the (undoped) crystals of this family, the anion-anion overlap is at least one order of magnitude smaller than the anion-cation overlap. In the crystals of the B_1 and B_2 families there are bond critical points between anions, so that the effective local coordination is 6 for cations and 18 for anions (6 anion-cation and 12 anion-anion bonds).[65] In the B_1 crystals (excepting NaI) we have found that the anion-anion overlap is smaller but of the same order of magnitude than cation-anion overlap. In the B_2 crystals, and also in NaI, anion-anion overlap is the largest contribution to the repulsive interactions, and thus anion-cation contacts are less important. The cations of the B_2 family occupy the interstitial holes left in the anionic fcc sublattice. It is then not surprising that when the cation-anion overlap is not so important, the expansion of the cation shell is an exception to the general trends; it is, in fact, nearly constant for the B_2 family.

Let us turn to discuss the distortion of the second and third shells. In all cases, the second shell suffers a contraction of a small magnitude compared to the large expansion of the first shell. In Figure 1 one can see that the radial outward motion of the first cation shell is not going to affect much the positions of the twelve anions of shell 2, so it becomes understandable that the anions of that shell move little. The small contraction of the second shell optimizes the Madelung energy around the impurity and also serves to pack more efficiently the ions in response to the outward motion of the cations. The quantitative trend of that contraction is understood with reference to the three topological families discussed in the previous paragraph and their relation to the anion-anion overlap: the contraction is largest for those crystals where the anion-anion overlap is small (R_1 crystals), intermediate when that overlap begins to count (B_1 crystals), and finally, it is lowest for the B_2 crystals, where anion-anion contacts are important. This explains the trends observed: if the anion is fixed, the contraction is larger the larger the cation size, because the Ag^--X^- overlap decreases with increasing cation size. On the other hand, if the cation is fixed, in Rb, K, and Na salts the contraction decreases with increasing anion size, because the Ag^--X^- overlap increases with anion size. But in Li salts the trend is inverted because Ag^--X^- overlaps decrease with anion size. The distortion of the third shell is not directly related to the introduction of the impurity, as the overlap between the cations of that shell and Ag^- is very small (see Fig. 1). The expansion of this shell appears to be again of a purely electrostatic origin. The relative values of the displacements (R_3 - $R_3^{crystal}$)/$R_3^{crystal}$ are very small, less than 1 % except in LiF.

The ΔR_4 displacements, always an expansion, proceed along the same crystallographic direction as the ΔR_1 displacements. Thus, the expansion is clearly induced by the expansion of the first shell. The relative displacements (R_4-$R_4^{crystal}$)/$R_4^{crystal}$ adopt values between 1 % and 5%, compared to values of 9–15 % for (R_1-$R_1^{crystal}$)/$R_1^{crystal}$. These numbers indicate that the expansion of the (ninth) shell formed by six cations at ($\frac{3}{2}$,0,0) is not expected to be higher than 1 %. In the K and Rb salts ΔR_4 is larger when ΔR_1 is larger, while in Li and Na salts ΔR_4 and ΔR_1 are both almost independent of the anion, so the displacements of the first and fourth shells are correlated. If the anion is fixed, the expansion increases with the cation size, and no special behaviour is observed in the cases of LiCl, LiBr, LiI and NaI.

We conclude that the lattice relaxation around the substitutional impurity in the alkali halides involves the concerted movement of several coordination shells. However, it is not yet clear from the results presented up to this point whether the lattice relaxations of the second, third and fourth shells have a substantial influence on the energy of formation of the defect. At low pressure and temperature conditions, the formation of the impurity centers should be discussed in terms of the internal energy difference for the exchange reaction[21]

$$(X^- : AX)_s + Imp_g^- \rightleftharpoons (Imp^- : AX)_s + X_g^-, \qquad (3)$$

where the s and g subindexes refer to solid and gas phases, respectively. In order to establish the importance of the relaxation of the lattice beyond the first coordination shell, we have calculated the formation energy ΔH of the defects by employing two different models for the active cluster, shown in Fig. 1: one of them is that formed by 179 ions described in section II; the other includes just four coordination shells around the central ion (a total of 33 ions), and only the positions of the six ions in the first coordination shell are allowed to relax. The results are shown in Table IV. We see that according to the small cluster model the energy of formation of the defects is always positive, that is none of the impurity centers are stable centers. Enlarging the cluster size to include a self-consistent treatment of 179 ions and extending the lattice relaxation up to the fourth coordination shell induces a huge stabilization of all the impurity centers. The trend

of ΔH is simple. For a given impurity (Ag^- or Cu^-) the heat of formation decreases by increasing the atomic number of the cation (alkali) or of the anion (halogen). The positive value of ΔH in the calculation for the small cluster is understandable: the impurity simply pushes its neighbor cations producing a high elastic strain energy since the rest of the lattice is not allowed to respond. In the second model three more shells are allowed to move in response to that initial stress and the relaxation lowers the elastic energy so much that the electronic contributions turn ΔH negative in all cases except Ag^-:LiF and Ag^-:NaF (ΔH is nearly zero in Ag^-:LiCl). It is useful to notice that ΔR_1, the displacement of the first shell, is lower for the first cluster model compared to the second. This means that due to the constraints imposed by the first model the atoms of the first shell are unable to reach their preferred equilibrium positions in the presence of the impurity, a fact that is consistent with the large calculated ΔH. The change of sign in ΔH can be interpreted as suggesting that most of the elastic relaxation of the lattice has been accounted for and that allowing for the elastic relaxation of more shells will have a minor effect. The two cases with a positive ΔH, Ag^-:LiF and Ag^-:NaF, are still intriguing. These two crystals have the smallest lattice parameters within the whole family studied here, and it is conceivable that the elastic effects will be largest. The question if the relaxation of more coordination shells is able to stabilize those two systems deserves further investigation.

As indicated above the difference in the heats of formation given by the two models, ΔH(model 2) - ΔH(model 1), gives a measure of the lowering of elastic strain when more coordination shells are allowed to relax. From Table IV one can verify that, for a given crystal, this energy is essentially independent of the impurity, while both ΔH(model 1) and ΔH(model 2) depend on the impurity. This confirms our interpretation of the effect of allowing for the elastic relaxation of several shells: that relaxation is mainly a host effect.

IV. SUMMARY

We have reported a study of the local lattice distortions induced by substitutional Ag^- and Cu^- impurities in the family of alkali halide crystals excepting those containing cesium. For this purpose, the *ab initio* Perturbed Ion (PI) model has been used. A large active cluster of 179 ions, embedded in an accurate quantum environment representing the rest of the crystal, has been studied. The local distortions obtained extend beyond the first shell of neighbors in all cases. Thus, the assumptions frequently employed in impurity calculations, which consider the active space as formed by the central impurity plus its first coordination shell only, should be taken with some care. Distortion trends have been identified and discussed. The first coordination shell (cations) around the impurity experiences an expansion as a consequence of the larger size of the impurity anion compared to the halogens. That expansion is larger for the Ag^- than for the Cu^- impurity, also because the first anion is larger than the second. The trends can be qualitatively explained by considering the difference in size between the impurity and the substituted anion in all cases except in those crystals with a very small size ratio between cation and anion. In those cases, that is for LiCl, LiBr, LiI and NaI, anion-anion contacts are important. Those four materials have been found to exhibit special behavior in a number of previous studies involving crystals and clusters. The contraction of the second shell as well as the expansion of the third shell are small and arise from a combination of electrostatic and packing origins. The fourth shell experiences a substantial expansion as a consequence of the direct pushing induced by the expansion of the first shell. The analysis of the energies of formation of the defects clearly shows that elastic relaxation of several coordination shells around the impurity is necessary in the modeling of these materials since this affects even the sign of the energy of formation.

Acknowledgements: Work supported by DGES (PB98-0345) and Junta de Castilla y León (VA28/99). A. Aguado is grateful to University of Valladolid for financial support. We thank the suggestions of one referee.

Captions of Tables

Table I. Radial displacements ΔR_i (see eq. (1)), in Å, of the first four shells of ions around the silver and copper impurities.

Table II. $(< r^2 >)^{1/2}$, where the expectation values are taken over the outermost orbital of the F^- anion in pure alkali fluorides and of the silver anion in Ag^--doped alkali fluorides. All quantities in Å.

Table III. Difference of radii between Ag^- and the substituted anion (see eq. (2)), in Å.

Table IV. Formation energies (in eV) of copper and silver substitutional centers in different alkali halide host lattices, calculated employing two different models for the active cluster. First row: the active cluster contains 33 ions, and only the positions of the ions in the first coordination shell are allowed to relax. Second row: the active cluster contains 179 ions, and the positions of the ions in the first four coordination shells are allowed to relax.

Captions of Figures

Figure 1. The active cluster $(ImpA_{92}X_{86})^{5+}$ employed to represent the region around the impurity, where Imp=Ag, Cu; light spheres are cations and dark spheres anions. The core of the cluster, formed by the four first coordination shells, which are allowed to breath, is also indicated separately.

Figure 2. Shell distortions ΔR_i (i=1,2,3,4) around Ag^-, plotted as a function of cation size.

[1] G. Blasse and B. C. Grabmaier, *Luminescent materials*, Springer Verlag, Berlin (1995).
[2] J. H. Barkyoumb and A. N. Mansour, Phys. Rev. B **46**, 8768 (1992).
[3] W. F. Pong, R. A. Mayanovic, B. A. Bunker, J. K. Furdyna, and U. Debska, Phys. Rev. B **41**, 8440 (1990).
[4] C. Zaldo, C. Prieto, H. Dexpert, and P. Fessler, J. Phys.: Condens. Matter **3**, 4135 (1991).
[5] M. J. Puska, S. Pöykkö, M. Pesola, and R. M. Nieminen, Phys. Rev. B **58**, 1318 (1998).
[6] H. Chermette and C. Pedrini, J. Chem. Phys. **75**, 1869 (1981).
[7] N. W. Winter, R. M. Pitzer, and D. K. Temple, J. Chem. Phys. **86**, 3549 (1987).
[8] A. B. Kunz and J. M. Vail, Phys. Rev. B **38**, 1058 (1988).
[9] Z. Barandiarán and L. Seijo, J. Chem. Phys. **89**, 5739 (1988).
[10] V. Luaña and L. Pueyo, Phys. Rev. B **39**, 11093 (1989).
[11] V. Luaña, M. Bermejo, M. Flórez, J. M. Recio, and L. Pueyo, J. Chem. Phys. **90**, 6409 (1989).
[12] L. Seijo and Z. Barandiarán, J. Chem. Phys. **94**, 8158 (1991).
[13] J. Andriessen, P. Dorenbos, and C. W. E. van Eijk, Mol. Phys. **74**, 535 (1991).
[14] M. S. Islam and R. C. Baetzold, J. Phys. Chem. Solids **53**, 1105 (1992).
[15] V. Luaña and M. Flórez, J. Chem. Phys. **97**, 6544 (1992).
[16] E. Miyoshi and S. Huzinaga, Phys. Rev. B **48**, 8583 (1993).
[17] A. Scacco, S. Fioravanti, M. Missori, U. M. Grassano, A. Luci, M. Palummo, E. Giovenale, and N. Zema, J. Phys. Chem. Solids **54**, 1035 (1993).
[18] V. Luaña, M. Flórez, and L. Pueyo, J. Chem. Phys. **99**, 7970 (1993).
[19] R. Visser, J. Andriessen, P. Dorenbos, and C. W. E. van Eijk, J. Phys.: Condens. Matter **5**, 5887 (1993).
[20] J. Andrés, A. Beltrán, S. Bohm, A. Flores-Riveros, J. A. Igualada, V. Luaña, A. Martín Pendás, and G. Monrós, J. Phys. Chem. **97**, 2555 (1993).
[21] M. Flórez, M. A. Blanco, V. Luaña, and L. Pueyo, Phys. Rev. B **49**, 69 (1994).
[22] A. Beltrán, A. Flores-Riveros, J. Andrés, V. Luaña, and A. Martín Pendás, J. Phys. Chem. **98**, 7741 (1994).
[23] M. Berrondo and J. F. Rivas-Silva, Int. J. Quantum Chem. Quantum. Chem. Symp. **29**, 253 (1995).
[24] J. L. Pascual and L. Seijo, J. Chem. Phys. **102**, 5368 (1995).
[25] T. J. Gryk and R. H. Bartram, J. Phys. Chem. Solids **56**, 863 (1995).
[26] R. Llusar, M. Casarrubios, Z. Barandiarán, and L. Seijo, J. Chem. Phys. **105**, 5321 (1996).
[27] L. Seijo and Z. Barandiarán, Int. J. Quantum Chem. **60**, 617 (1996).
[28] M. Berrondo, F. Rivas-Silva, and J. B. Czirr, *Proceedings of the International Conference on Inorganic Sintillators and their Applications, SCINT95*. Delft University Press (1996), p. 144.
[29] M. Berrondo and F. Rivas-Silva, Int. J. Quantum Chem. **57**, 1115 (1996).
[30] J. F. Rivas-Silva, A. Flores-Riveros, A. Ayuela, and M. Berrondo, Computational Materials Science **11**, 150 (1998).
[31] A. Aguado, A. Ayuela, J. M. López, and J. A. Alonso, Phys. Rev. B **58**, 11964 (1998).
[32] M. T. Barriuso, J. A. Aramburu, and M. Moreno, J. Phys.: Condens. Matter **11**, L525 (1999).
[33] S.Huzinaga, L. Seijo, Z. Barandiarán, and M. Klobukowski, J. Chem. Phys. **86**, 2132 (1987).
[34] X. Zhang and C. R. A. Catlow, Phys. Rev. B **47**, 5315 (1993).
[35] X. Zhang, C. K. Ong, and A. M. Stoneham, J. Phys.: Condens. Matter **6**, 5647 (1994).
[36] M. S. Islam and R. C. Baetzold, J. Mater. Chem. **4**, 299 (1994).
[37] M. S. Islam and L. J. Winch, Phys. Rev. B **52**, 10510 (1995).
[38] D. C. Sayle, C. R. A. Catlow, M. -A. Perrin, and P. Nortier, J. Phys. Chem. Solids **56**, 799 (1995).
[39] M. J. Akhtar, Z. D. N. Akhtar, R. A. Jackson, and C. R. A. Catlow, J. Am. Chem. Soc. **78**, 421 (1995).
[40] M. Exner, H. Donnerberg, C. R. A. Catlow, and O. F. Schirmer, Phys. Rev. B **52**, 3930 (1995).
[41] C. R. A. Catlow, M. S. Islam, and X. Zhang, J. Phys.: Condens. Matter **10**, L49 (1998).
[42] C. R. A. Catlow and P. D. Townsend, *Point Defects in Materials*, Academic Press, London (1998).
[43] A. M. Stoneham, *Handbook of Interatomic Potentials I: Ionic Crystals*, UKAEA report AERE-R 9598 (1981).
[44] J. H. Harding, Rep. Prog. Phys. **53**, 1403 (1990).
[45] M. Wilson and P. A. Madden, J. Phys.: Condens. Matter **5**, 2687 (1993).
[46] M. Wilson, P. A. Madden, N. C. Pyper, and J. H. Harding, J. Chem. Phys. **104**, 8068 (1996).
[47] J. D. Gale, Phil. Mag. B **73**, 3 (1996).
[48] J. D. Gale, Faraday Discuss. **106**, 219 (1997).
[49] V. Luaña and L. Pueyo, Phys. Rev. B **41**, 3800 (1990).
[50] V. Luaña, J. M. Recio, and L. Pueyo, Phys. Rev. B **42**, 1791 (1990).
[51] L. Pueyo, V. Luaña, M. Flórez, and E. Francisco, in *Structure, Interactions and Reactivity*, edited by S. Fraga (Elsevier, Amsterdam, 1992), vol. B, p. 504
[52] V. Luaña, M. Flórez, E. Francisco, A. Martín Pendás, J. M. Recio, M. Bermejo, and L. Pueyo, in *Cluster Models for Surface and Bulk Phenomena*, edited by G. Pacchioni, P. S. Bagus and F. Parmigiani (Plenum, New York, 1992), p. 605
[53] V. Luaña, A. Martín Pendás, J. M. Recio, and E. Francisco, Comput. Phys. Commun. **77**, 107 (1993).
[54] S. Huzinaga and A. P. Cantu, J. Chem. Phys. **55**, 5543 (1971).
[55] S. Huzinaga, D. McWilliams, and A. A. Cantu, Adv. Quantum Chem. **7**, 183 (1973).
[56] C. C. J. Roothaan and P. S. Bagus, *Methods in Computa-*

tional Physics, vol. 2, 47 (Academic, New York, 1963).
[57] E. Francisco, A. Martín Pendás, and W. H. Adams, J. Chem. Phys. **97**, 6504 (1992).
[58] E. Clementi, IBM J. Res. Dev. **9**, 2 (1965).
[59] S. J. Chakravorty and E. Clementi, Phys. Rev. A **39**, 2290 (1989).
[60] W. H. Press and S. A. Teukolsky, Computers in Physics **5**, 426, (1991).
[61] E. Clementi and C. Roetti, At. Data and Nuc. Data Tables **14**, 177 (1974).
[62] N. M. Ashcroft and N. D. Mermin, *Solid State Physics* (Holt, Rinehart and Winston, New York, 1976).
[63] A. Martín Pendás, J. M. Recio, E. Francisco, and V. Luaña, Phys. Rev. B **56**, 3010 (1997).
[64] A. Aguado, A. Ayuela, J. M. López, and J. A. Alonso, Phys. Rev. B **56**, 15353 (1997).
[65] A. Martín Pendás, A. Costales, and V. Luaña, J. Phys. Chem. B **102**, 6937 (1998).
[66] R. F. W. Bader, *Atoms in Molecules* (Oxford University Press, Oxford, 1990).

[

Crystal	Ag^-	Cu^-	Crystal	Ag^-	Cu^-	Crystal	Ag^-	Cu^-	Crystal	Ag^-	Cu^-
LiF	0.288	0.267	LiCl	0.294	0.290	LiBr	0.299	0.294	LiI	0.308	0.302
	-0.0416	-0.0371		-0.0439	-0.0403		-0.0478	-0.0467		-0.0492	-0.0484
	0.0418	0.0397		0.0439	0.0425		0.0462	0.0452		0.0457	0.0446
	0.0687	0.0619		0.0622	0.0617		0.0642	0.0636		0.0732	0.0732
NaF	0.308	0.292	NaCl	0.289	0.285	NaBr	0.290	0.284	NaI	0.299	0.288
	-0.0660	-0.0621		-0.0628	-0.0620		-0.0600	-0.0591		-0.0552	-0.0540
	0.0336	0.0336		0.0350	0.0350		0.0388	0.0383		0.0401	0.0404
	0.121	0.114		0.107	0.100		0.0867	0.0843		0.0915	0.0797
KF	0.364	0.355	KCl	0.326	0.315	KBr	0.311	0.300	KI	0.284	0.269
	-0.0778	-0.0695		-0.0739	-0.0686		-0.0719	-0.0709		-0.0709	-0.0699
	0.0319	0.0314		0.0316	0.0316		0.0313	0.0307		0.0318	0.0312
	0.224	0.220		0.205	0.200		0.172	0.166		0.145	0.136
RbF	0.416	0.408	RbCl	0.351	0.343	RbBr	0.332	0.318	RbI	0.300	0.281
	-0.0828	-0.0736		-0.0749	-0.0731		-0.0728	-0.0728		-0.0727	-0.0716
	0.0307	0.0292		0.0268	0.0262		0.0261	0.0261		0.0286	0.0286
	0.254	0.249		0.226	0.220		0.195	0.187		0.166	0.156

Crystal	$(< r^2 >)^{1/2}(F^-)$	$(< r^2 >)^{1/2}(Ag^-)$
LiF	0.698	1.303
NaF	0.704	1.343
KF	0.710	1.380
RbF	0.712	1.401

Crystal	δ	Crystal	δ	Crystal	δ	Crystal	δ
LiF	0.605	LiCl	0.343	LiBr	0.273	LiI	0.162
NaF	0.639	NaCl	0.388	NaBr	0.328	NaI	0.209
KF	0.670	KCl	0.401	KBr	0.368	KI	0.241
RbF	0.689	RbCl	0.460	RbBr	0.378	RbI	0.251

Crystal	Ag^-	Cu^-	Crystal	Ag^-	Cu^-	Crystal	Ag^-	Cu^-	Crystal	Ag^-	Cu^-
LiF	16.79	15.41	LiCl	11.62	11.04	LiBr	11.63	11.02	LiI	9.76	9.30
	1.29	-0.22		0.02	-0.57		-0.21	-0.64		-0.61	-1.10
NaF	13.38	12.44	NaCl	11.20	10.63	NaBr	10.38	9.91	NaI	8.68	8.52
	0.45	-0.55		-0.02	-0.63		-0.24	-0.87		-0.85	-1.01
KF	11.25	10.42	KCl	9.85	9.32	KBr	9.08	8.69	KI	7.82	7.55
	-0.33	-1.14		-0.84	-1.28		-1.04	-1.26		-1.11	-1.20
RbF	10.37	9.60	RbCl	9.19	8.73	RbBr	8.76	8.39	RbI	7.56	7.31
	-0.57	-1.31		-0.91	-1.38		-0.97	-1.35		-1.09	-1.35

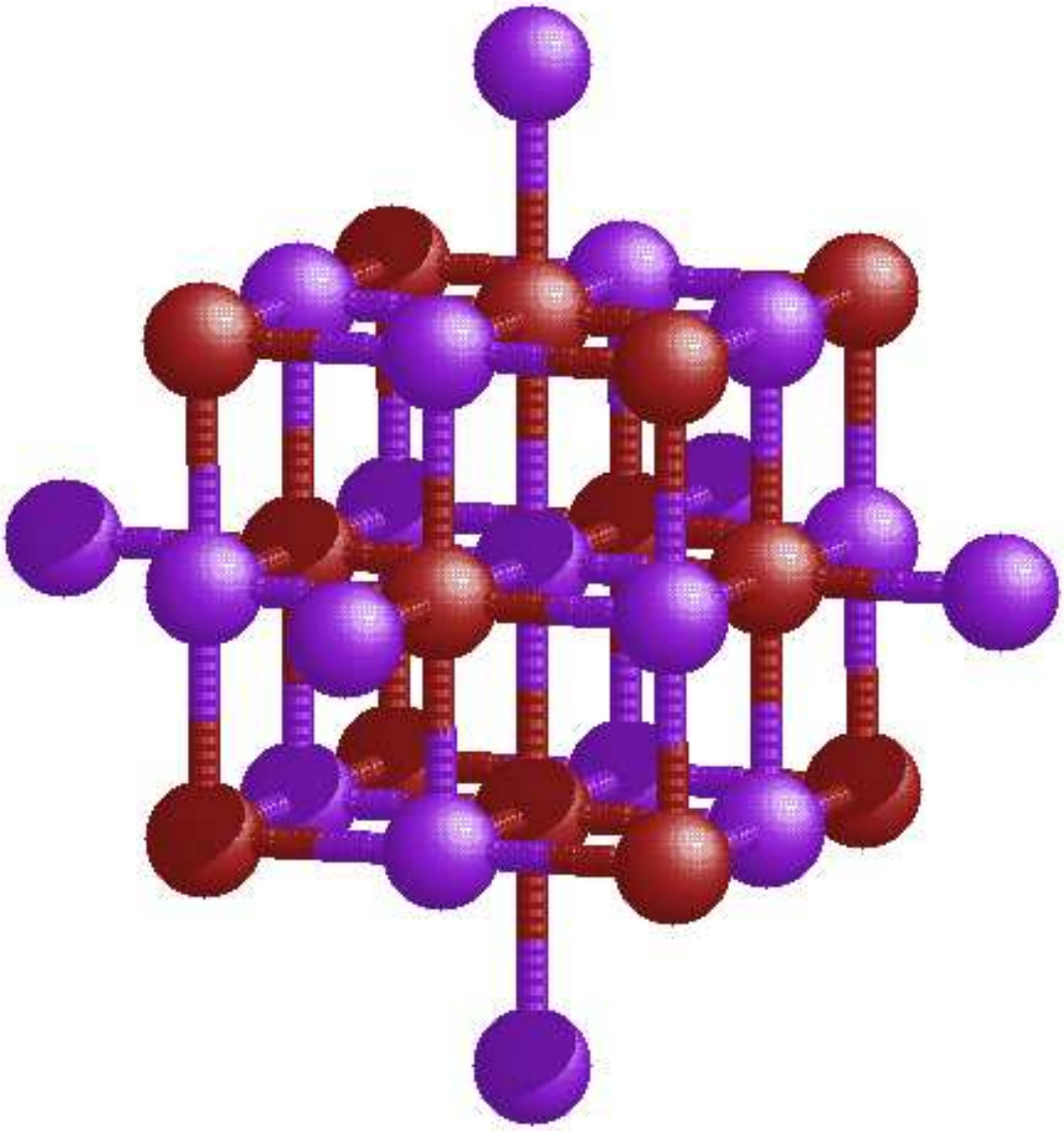

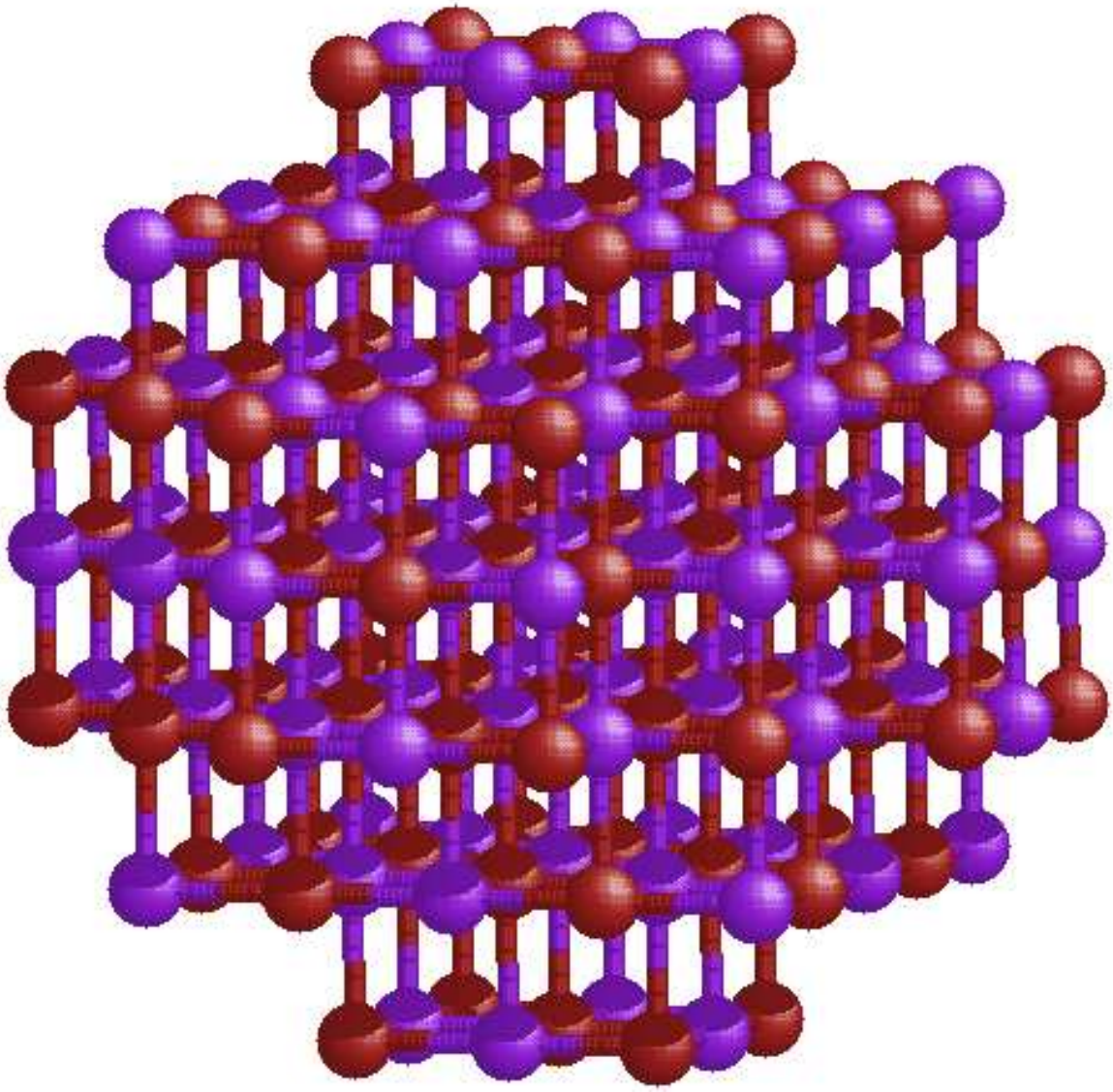

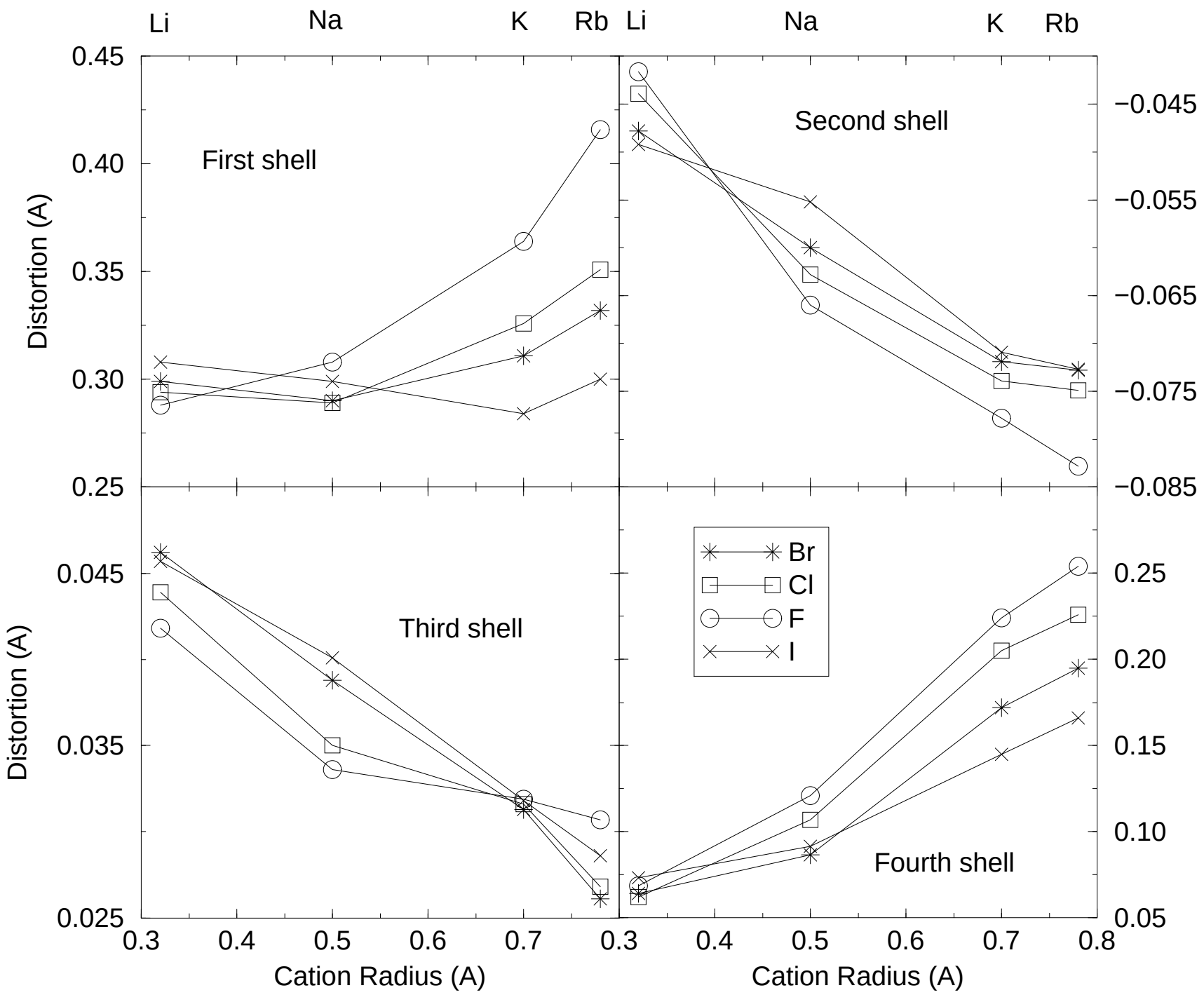
Li
Na
K
Rb
Li
Na
K
Rb
First shell
Second shell
Third shell
Fourth shell
Br
Cl
F
I
Distortion (A)
Distortion (A)
Cation Radius (A)
Cation Radius (A)
0.45
0.40
0.35
0.30
0.25
−0.045
−0.055
−0.065
−0.075
−0.085
0.045
0.035
0.025
0.25
0.20
0.15
0.10
0.05
0.3
0.4
0.5
0.6
0.7
0.3
0.4
0.5
0.6
0.7
0.8